Benzothiadiazole Functionalized D-A Type Covalent Organic Frameworks for Effective Photocatalytic Reduction of Aqueous Chromium (VI)

Weiben Chen,[a] Zongfan Yang,[a] Zhen Xie,[a] Yusen Li,[a] Xiang Yu[b] Fanli Lu,[a] and Long Chen[a]*

[a]*Department of Chemistry and Tianjin Key Laboratory of Molecular Optoelectronic Science, Tianjin University, Tianjin 300072, China*

[b]*Analytical and Testing Center, Jinan University, Guangzhou 510632, China*

*E-mail: long.chen@tju.edu.cn (L. Chen)

Contents

Section 1. Materials and Methods

o-dichlorobenzene (o-DCB), *n*-butanol (n-BuOH) were purchased from Aladdin industrial corporation, Shanghai, China. 1,5-Diphenylcarbohydrazide was obtained from Adamas Reagent, Ltd. All the commercial chemicals were directly used as received without further purification.

^{1}H and ^{13}C NMR spectra of all monomers were carried out on a Bruker AVANCE III-400MHz NMR spectrometer. The ^{13}C CP/MAS NMR spectra were obtained on Varian Infinityplus 300 (300MHz) solid-state NMR spectrometer. Fluorescence measurement were performed on a Hitachi F-7000 fluorescence spectrophotometer. Elemental analyses were carried out on Elementar model Vario Micro analyzer. Thermogravimetric analysis (TGA) of BT-COFs were evaluated in TA instrumentsTGA-Q50-1918 analyzer from room temperature to 800 ^{o}C under N_2 atmosphere with a heating rate of 10 ^{o}C/min. The Powder X-ray diffraction (PXRD) patterns were obtained on RIGAKU SMARTLAB-9KW with a Cu-target tube and a graphite monochromator. Transmission electron microscopies (TEM) and high-resolution transmission electron microscopies (HR-TEM) were performed on a FEI model Tecani 20 microscope and a JEOL model JSM-2100F. Field emission scanning electron microscopies (FE-SEM) were carried out using a JEOL model JSM-6700 microscope operating at an accelerating voltage of 5.0 kV. The nitrogen adsorption and desorption were measured by using a Bel Japan Inc. model BELSOPR-mini II analyser and the samples were degassed at 100 ^{o}C for 3 h under vacuum (10^{-5} bar) before analysis. The pore size distribution was calculated from the adsorption branch with the nonlocal density functional theory (NLDFT). X-ray photoelectron spectroscopy (XPS) was performed using 65 HP 5950A with Mg Kα as the source and the C 1s peak at 284.6 eV as an internal standard.

Electrochemical Characterization. CHI-660E electrochemical workstation (CH Instruments, USA) with three-electrode system was used to determine electrochemical measurements (working electrode: the glass carbon electrode (GCE), counter electrode: platinum wire electrode, and reference electrode: saturated calomel electrode (SCE)).

To create measurable COF films, the BT-COF (2 mg) was mixed with 5 wt % Nafion (20 μl) and ethanol (490 μl) and ultrasonic for 30 min. The glassy carbon working electrode was painted with the mixture, and the solvents were evaporated in a vacuum oven for 12 h. The measurements were carried out in tetrabutylammonium phosphate (0.1 M) in acetonitrile. A Pt counter electrode and a SCE reference electrode were used. Scan rate: 100 mV/s, T = 25 ^{o}C.

For the transient photocurrent measurements, the COFs electrodes were obtained by adding 5 mg photocatalyst in 0.5 mL distilled water, and then the suspensions were sonicated for 15 min. To the slurries were added the 5 wt % Nafion solution (20 μl) and then sonicated for another 60 min. The obtained slurries were dropped on the ITO electrode (surface area *ca.* 1 x 1 cm^2) and dried in air for 12 h. The photocurrent measurements were performed at -0.4 V bias voltage in Na_2SO_4 (0.5 M) solution.

Section 2. Synthetic Procedures

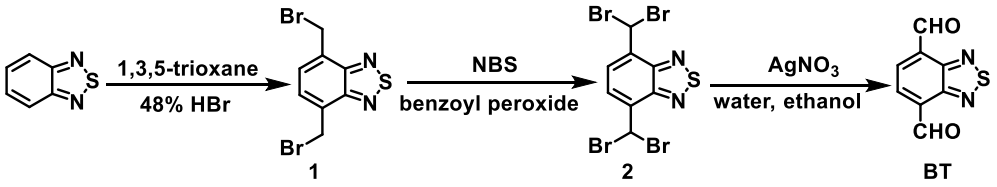

Scheme S1. Synthetic routes of benzo[c][1,2,5]thiadiazole-4,7-dicarbaldehyde.

4,7-Bis(bromomethyl)benzo[c][1,2,5]thiadiazole (1): To the stirred solution of 2,1,3-benzothiadiazole (5.0 g, 36.8 mmol) in 48% aqueous hydrobromic acid (HBr, 100 mL) and glacial acetic acid (60 mL) were added 1,3,5-trioxane (10.0 g, 111 mmol) and trimethyl(tetradecyl)ammonium bromide (1.0 g, 3 mmol). The solution was heated to refluxed for 24 h. After cooling to room temperature, the reaction mixture was poured to ice/water mixture, filtered and washed with water and ethanol and then dried under vacuum to afford compound as a white solid. Yield: (7.8 g, 63%). ^{1}H NMR ($CDCl_3$, 400 MHz) δ (ppm) = 7.63 (s, 2 H), 4.97 (d, 4 H).

Benzo[c][1,2,5]thiadiazole-4,7-dicarbaldehyde (BT): To a mixture of compound **1** (3.0 g, 9.0 mmol) and N-bromosuccinimide (NBS) (4.4 g, 37.3 mmol) in tetrachloromethane (30 ml) was added benzoyl peroxide (70 mg, 0.3 mmol). The mixture was heated under reflux for 24 h. The reaction mixture was cooled to room temperature. Afterward, the mixture was filtered and then dried under vacuum to give an off-white solid **2**. ^{1}H NMR ($CDCl_3$, 400 MHz), δ (ppm) = 8.12 (2H, s), 7.44 (2H, s). Without further purification, to a refluxed solution of the compound **2** (4 g, 16.8 mmol) in ethanol (100 mL) was added a solution of silver nitrate (6.0 g, 35.3 mmol) in 5 mL water. The mixture was heated under reflux for 24 h. The reaction mixture was cooled to room temperature. The solid salts were filtered and washed by water and ethanol. The solvent in filtrate was eliminated by rotary evaporator to give the yellow solid. The residue was purified with silica gel column chromatography to give compound BT as pale yellow solid. Yield: (420 mg, 52%).^{1}H NMR ($CDCl_3$, 400 MHz) δ (ppm) = 10.93 (2H, s), 8.36 (2H, s).

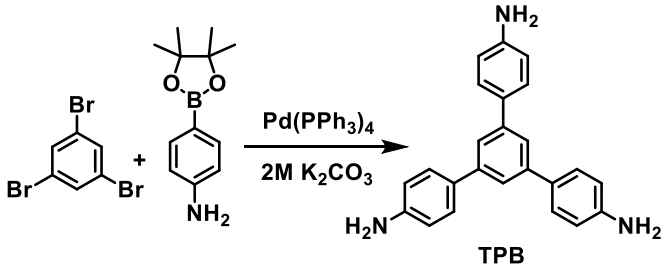

Scheme S2. Synthetic routes of 1,3,5-tris(4-aminophenyl)benzene.

1,3,5-tris(4-aminophenyl)benzene (TPB): 1,3,5-tribromobenzene (438 mg, 2 mmol) and 4-(4,4,5,5-tetramethyl-1,3,2-dioxaborolan-2-yl)aniline (190 mg, 6 mmol) were dissolved in 6 ml of DMF. Then, an aqueous K_2CO_3 (2 mL, 2.0 M) were added. After degassing by argon bubbling, tetrakis(triphenylphosphine)palladium(0) (35 mg, 0.03mmol) were added. The reaction mixture was heated to 100 °C for 24 h. The crude product was purified by column chromatography to afford an off-white solid. Yield (400 mg, 57%). ^{1}H NMR ($CDCl_3$, 400 MHz) δ (ppm) = 7.59 (s, 3H), 7.51 (d, J = 8.7 Hz, 6H), 6.77 (d, J = 8.7 Hz, 6H), 3.82 (s, 6H).

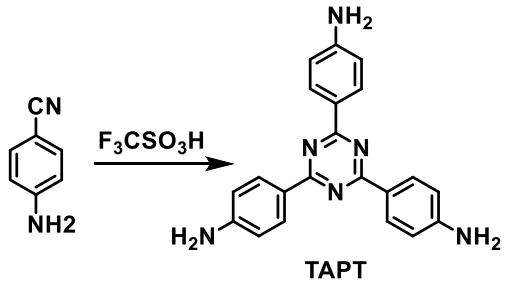

Scheme S3. Synthetic routes of 1,3,5-tris-(4-aminophenyl)triazine.

1,3,5-tris-(4-aminophenyl)triazine (TAPT): 4-aminobenzonitrile (772 mg, 6.54 mmol) was added to a two-neck round-bottom flask. Then, trifluoromethanesulfonic acid (4 mL, 44.4 mmol) was added dropwise under an inert atmosphere at 0 °C. The reaction mixture was stirred continuously at room temperature under inert conditions for 24 h. After the completion of the reaction, distilled water (40 mL) was poured into the final mixture, followed by an aqueous solution of sodium hydroxide for neutralization until the final pH value was approximately 7. Initially, a deep-orange precipitate appeared with increasing pH value under basic conditions. The mixture was extracted by ethyl acetate (20 mL×3). The organic phase was combined and the solvent was removal by reduce pressure evaporator. The pale-yellow residue was purified with silica gel column chromatography (petroleum : ethyl acetate = 1:1). Yield (434 mg, 56%). ^{1}H NMR ($CDCl_3$, 400 MHz) δ (ppm) = 8.34 (d, J = 8.5 Hz, 6H), 6.68 (d, J = 8.5 Hz, 6H), 5.88 (s, 6H).

TPB-BT-COF: A 10 mL Pyrex tube was charged with 1,3,5-tris(4-aminophenyl)benzene (20 mg, 0.057 mmol), benzo[c][1,2,5]thiadiazole-4,7-dicarbaldehyde (15.6 mg, 0.081 mmol) and o-dichlorobenzene/n-butyl alcohol (1:1 v/v, 1 mL). After the mixture was sonicated for 1 min, an orange suspension was obtained. Subsequently, 0.1 mL of acetic acid (3 M) were added. After the mixture was sonicated for another 1min again. Afterwards, the tube was flash frozen at 77 K using a liquid N_2 bath and degassed by three freeze-pump-thaw cycles, sealed under vacuum and then heated at 120 °C for 3 days. A deep orange-red precipitate was formed, which was collected by sucking filtration and washed with N, N-dimethylformamide, anhydrous ethanol, acetone, and dichloromethane, separately. The collected sample was dried

under vacuum for 24 h to give an orange red colored powder (30 mg, 92% isolated yield). IR (powder, cm^{-1}): 1690 (w), 1618 (w), 1596 (s), 1570 (m), 1504(s), 1441 (m), 1388 (m), 1260 (m), 1171(w), 1151(w), 823 (s). Elemental analysis (%): Anal. Calcd. For ($C_{72}H_{54}N_{12}S_3$) (theoretical formula for an infinite 2D COF): C, 73.83; H, 3.61; N, 14.35. Found: C, 69.42; H, 5.88; N, 12.09.

TAPT-BT-COF: A 10 mL Pyrex tube was charged with 1,3,5-tris-(4-aminophenyl)triazine (20 mg, 0.056 mmol), benzo[c][1,2,5]thiadiazole-4,7-dicarbaldehyde (15.6 mg, 0.081 mmol) and o-dichlorobenzene/n-butyl alcohol (1:1 v/v, 1 mL). After the mixture was sonicated for 1 min, an orange suspension solution was obtained. Subsequently, 0.1 mL of acetic acid (3 M) were added. After the mixture was sonicated for another 1 min again. Afterwards, the tube was flash frozen at 77 K using a liquid N_2 bath and degassed by three freeze-pump-thaw cycles, sealed under vacuum and then heated at 120 °C for 3 days. A deep orange precipitate was formed, which was collected by sucking filtration and washed with N, N-dimethylformamide, anhydrous ethanol, acetone, and dichloromethane, separately. The collected sample was dried under vacuum for 24 h to give a deep orange powder (32 mg, 98% isolated yield). IR (powder, cm^{-1}): 1690 (w), 1614 (w), 1689 (w), 1577 (m), 1500 (s), 1415 (s), 1358 (m), 1255 (m), 1173(m), 1142(m), 811 (s). Elemental analysis (%): Anal. Calcd. For ($C_{66}H_{48}N_{18}S_3$) (theoretical formula for an infinite 2D COF): C, 67.28; H, 3.08; N, 21.42. Found: C, 66.97; H, 4.97; N, 19.34.

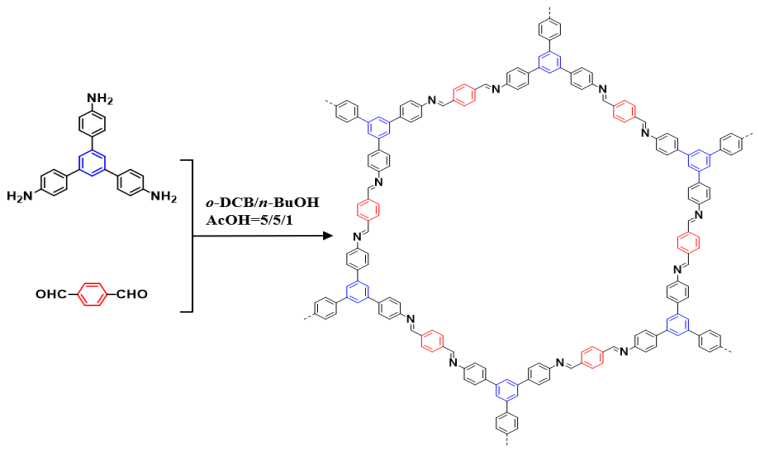

Scheme S4. synthetic routes of **TPB-TP-COF**.

TPB-TP-COF: A 10 mL Pyrex tube was charged with 1,3,5-tris(4-aminophenyl)benzene (28 mg, 0.08 mmol), terephthalaldehyde (16 mg, 0.11 mmol) and o-dichlorobenzene/n-butyl alcohol (1:1 v/v, 1 mL). After the mixture was sonicated for 1 min, an orange suspension solution was obtained. Subsequently, 0.1 mL of acetic acid (6 M) were added. After the mixture was sonicated for another 1 min again. Afterwards, the tube was flash frozen at 77 K using a liquid N_2 bath and degassed by three freeze-pump-thaw cycles, sealed under vacuum and then heated at 120 °C for 3 days. A bright yellow precipitate was formed, which was collected by sucking filtration and washed with N, N-dimethylformamide, anhydrous ethanol, acetone, and dichloromethane, separately. The collected sample was dried under vacuum for 24 h to give a bright yellow powder (35 mg, 88% isolated yield).

Section 3. ^{1}H NMR & ^{13}C NMR Spectra

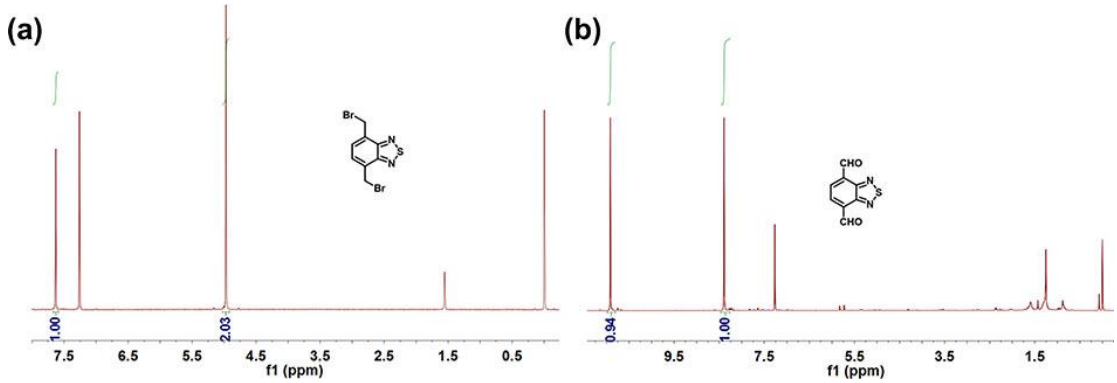

Figure S1. ^{1}H NMR (400 MHz, $CDCl_3$) spectra of (a) 4,7-Bis(bromomethyl)benzo[c][1,2,5]thiadiazole and (b) Benzo[c][1,2,5]thiadiazole-4,7-dicarbaldehyde (**BT**).

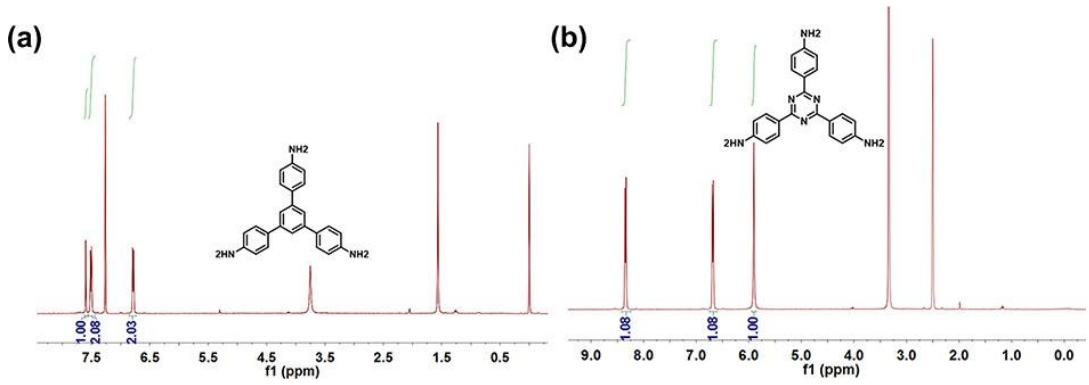

Figure S2. ^{1}H NMR (400 MHz, $CDCl_3$) spectra of (a) 1,3,5-tris(4-aminophenyl)benzene (**TPB**) and (b) 1,3,5-tris-(4-aminophenyl)triazine (**TAPT**).

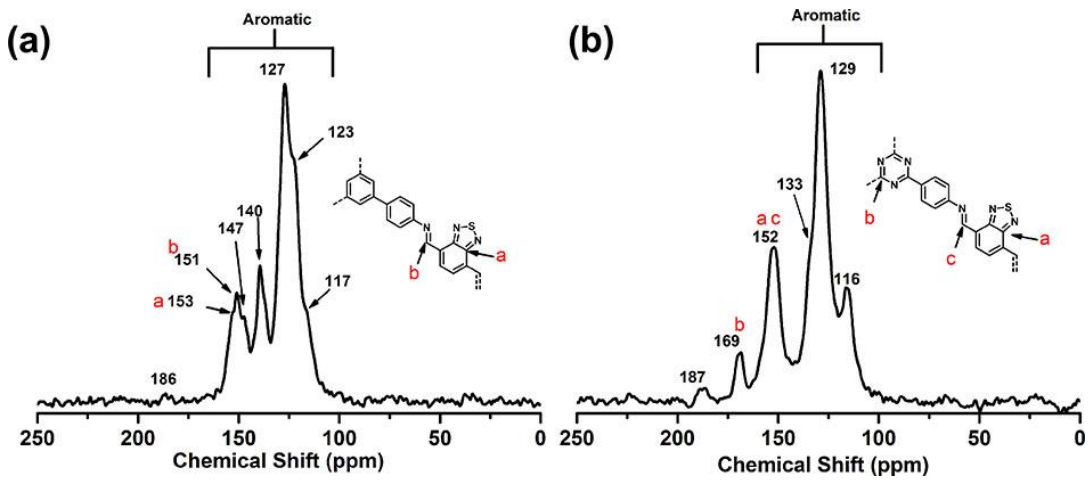

Figure S3. Solid state ^{13}C NMR spectra of (a) **TPB-BT-COF** and (b) **TAPT-BT-COF**.

Section 4. Elemental Analysis

Table S1. Elemental analysis of **TPB-BT-COF** and **TAPT-BT-COF**.

COFS		C	N	H
TPB-BT-COF	Anal. Calcd.	73.83%	14.35%	3.61%
	Found	69.42%	12.09%	5.88%
TAPT-BT-COF	Anal. Calcd.	67.28%	21.42%	3.08%
	Found	66.97%	19.34%	4.97%

Section 5. FT-IR Spectral Profiles

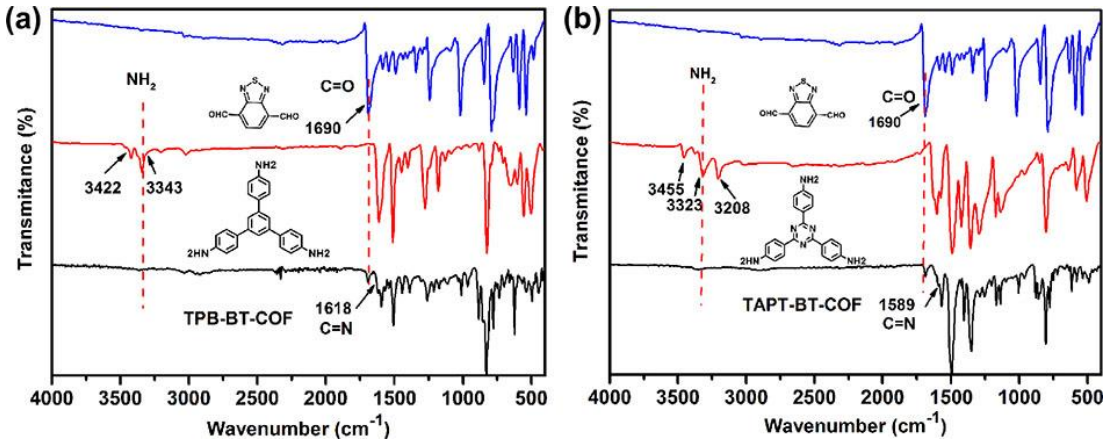

Figure S4. (a) FT-IR spectra comparison of the **TPB-BT-COF** (black line), monomer **TPB** (red line) and monomer **BT** (blue line); (b) FT-IR spectra comparison of the bulk **TAPT-BT-COF** (black line), **TAPT** (red line) and monomer **BT** (blue line).

Section 6. UV-visible Diffuse Reflectance Spectra

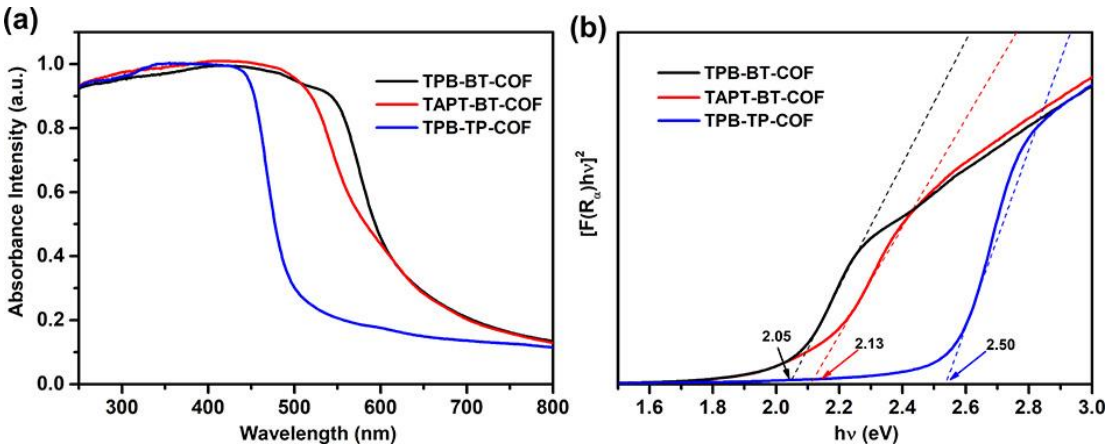

Figure S5. (a) UV-visible diffuse reflectance spectra and (b) Kubelka-Munk-transformed reflectance spectra of the bulk **TPB-BT-COF** (black curve), **TAPT-BT-COF** (red curve) and the control samples of **TPB-TP-COF** (blue) in the solid state

Section 7. Thermal Stability Analysis

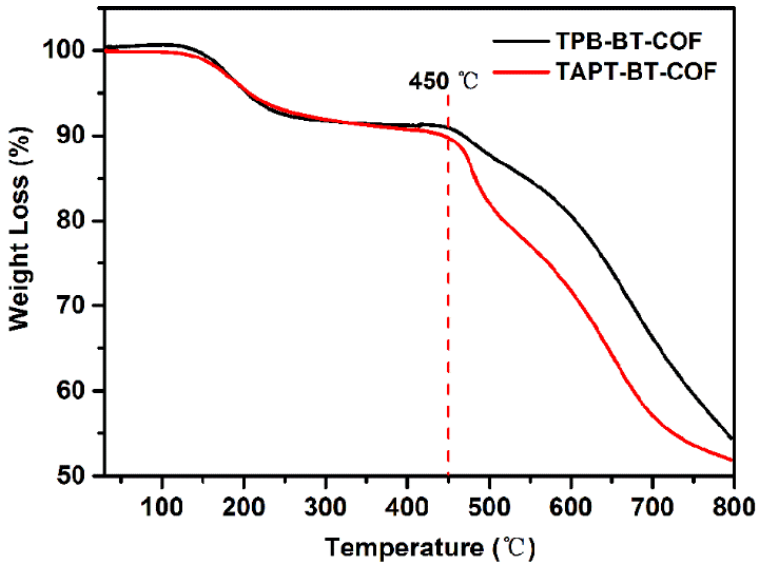

Figure S6. Thermogravimetric analysis (TGA) profiles of **TPB-BT-COF** (black) and **TAPT-BT-COF** (red) range from room temperature to 800 °C at 10 °C/min. TGA analysis indicated that both **TPB-BT-COF** and **TAPT-BT-COF** were thermally stable up to about 450 °C.

Section 8. Chemical Stability Tests

The typical procedure for the chemical stability tests of **BT-COFs** are described as follows.[S4] **BT-COFs** (15 mg) were as firstly dispersed in 2 mL of acetone. To the mixture was added 2 mL of an aqueous solution (pH =1 for hydrochloric acid aqueous solution and pH=13 for sodium hydroxide aqueous solution), and then the resulting suspension was kept for 12 h at room temperature. The resulted **BT-COFs** material was then isolated by centrifugation, washed with aqueous acetone solutions (V_{H2O}/Vacetone = 1/1, 3 ×6 mL) and THF, and then dried at room temperature under vacuum for 12 h. The structure of the dried **BT-COF** materials was then assessed via FT-IR spectroscopy and PXRD analysis. The results were shown in Figures S7 and S8, which indicate that **BT-COFs** are stable in aqueous solutions (pH = 1 and 13).

To the boiling water was added the **BT-COFs** (15 mg) and acutely stirred for 24 h. Subsequently, the solid reside were separated through the centrifugation and washed EtOH, THF, acetone, and then dried under vacuum for 12 h at room temperature. The results were shown in Figures S9 and S10, which indicate that **BT-COFs** are stable in the boiling water.

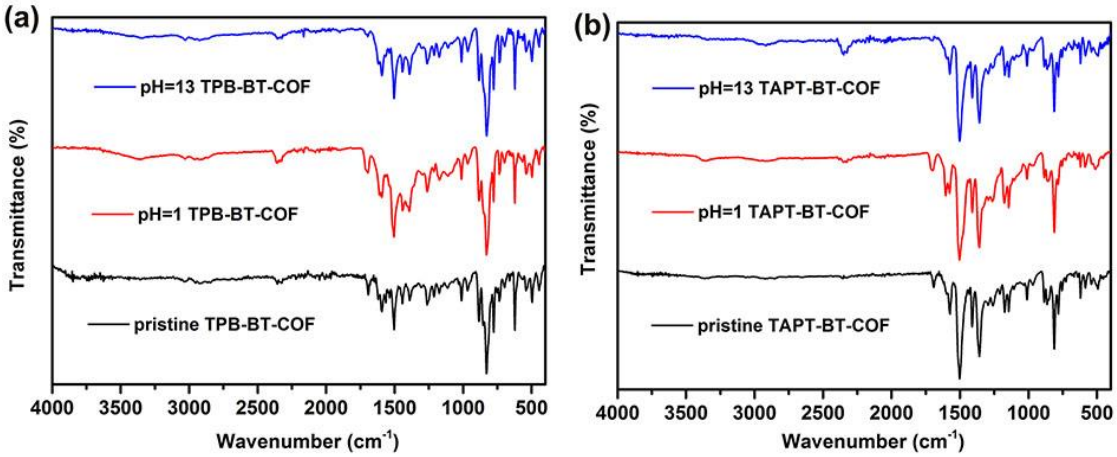

Figure S7. FT-IR spectra comparison of a) **TPB-BT-COF** and b) **TAPT-BT-COF** at different pH values.

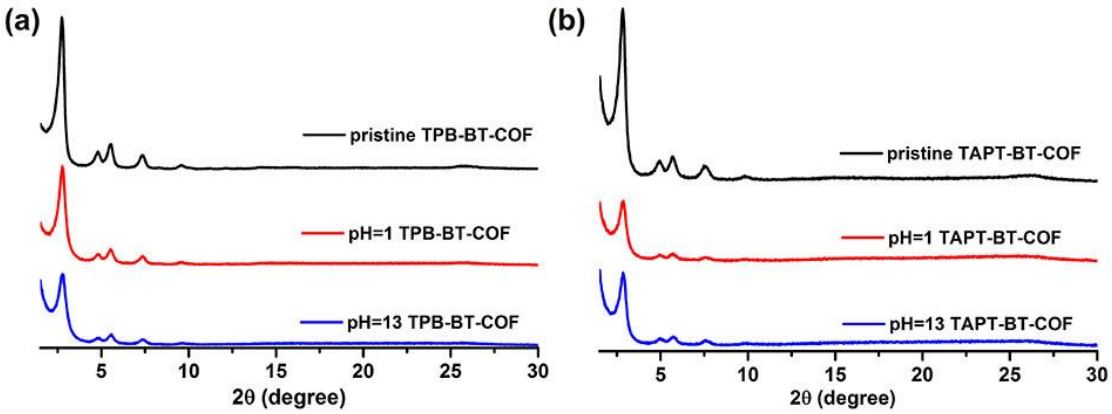

Figure S8. PXRD patterns of a) **TPB-BT-COF** and b) **TAPT-BT-COF** at different pH values.

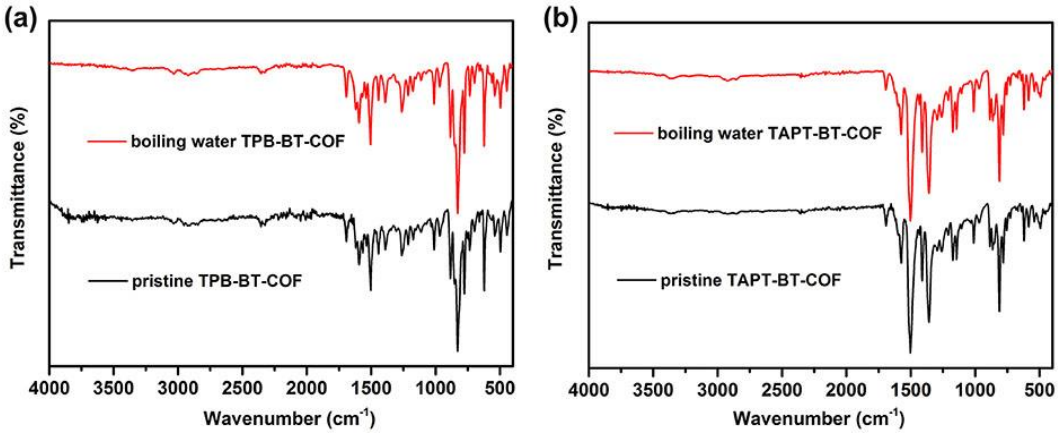

Figure S9. FT-IR spectra of BT-COFs before and after boiling water treatment: a) **TPB-BT-COF** and b) **TAPT-BT-COF**.

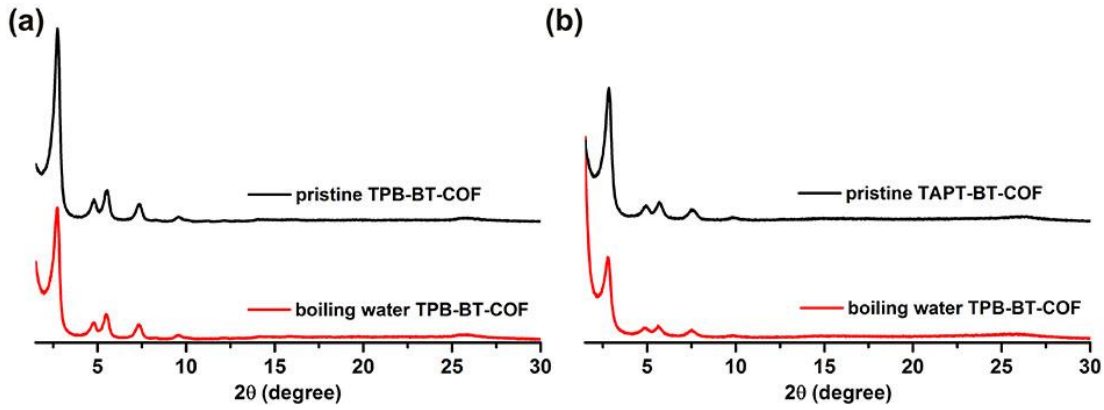

Figure S10. PXRD patterns of BT-COFs before and after boiling water treatment: a) **TPB-BT-COF** and b) **TAPT-BT-COF**.

Section 9. Photostability Tests

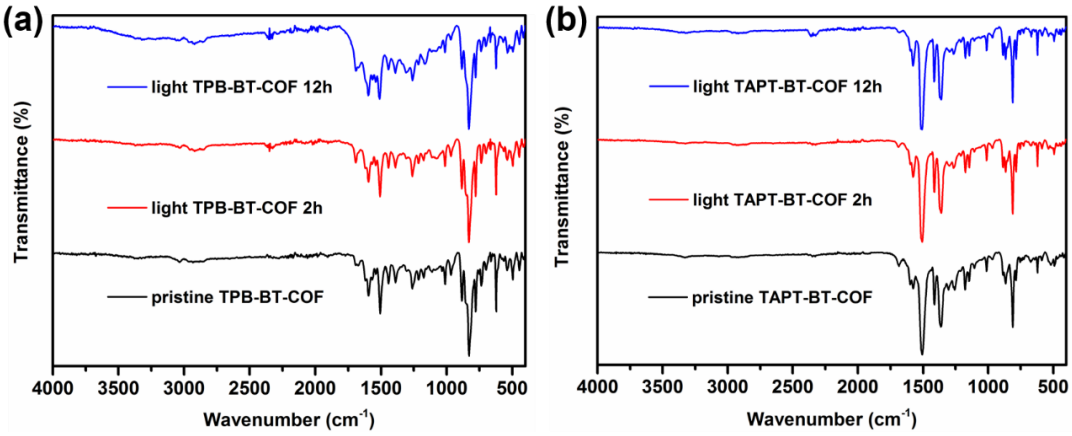

Figure S11. FT-IR spectra of a) **TPB-BT-COF** and b) **TAPT-BT-COF** in water for under visible light irradiation 2 h and 12 h.

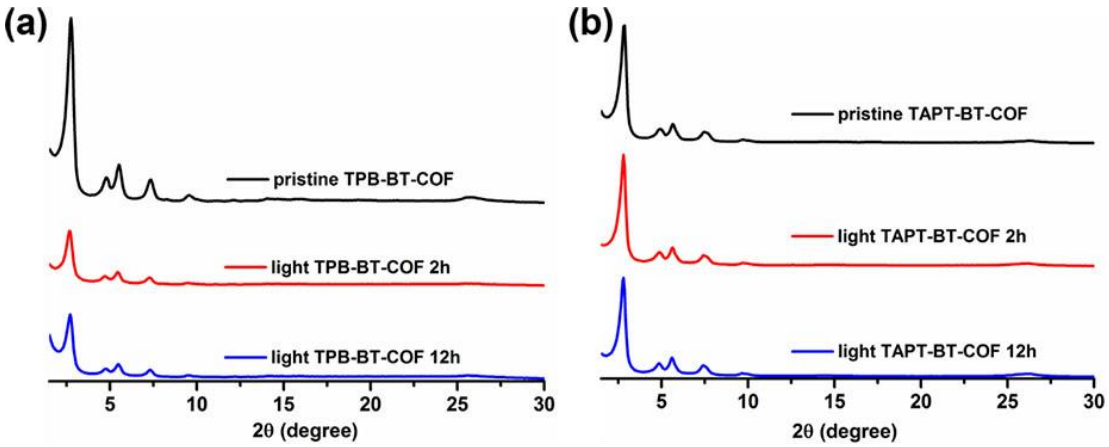

Figure S12. PXRD patterns of the bulk **TPB-BT-COF** and **TAPT-BT-COF** in water under visible light irradiation for 2 h and 12 h.

Section 10. Scanning Electron Microscopy

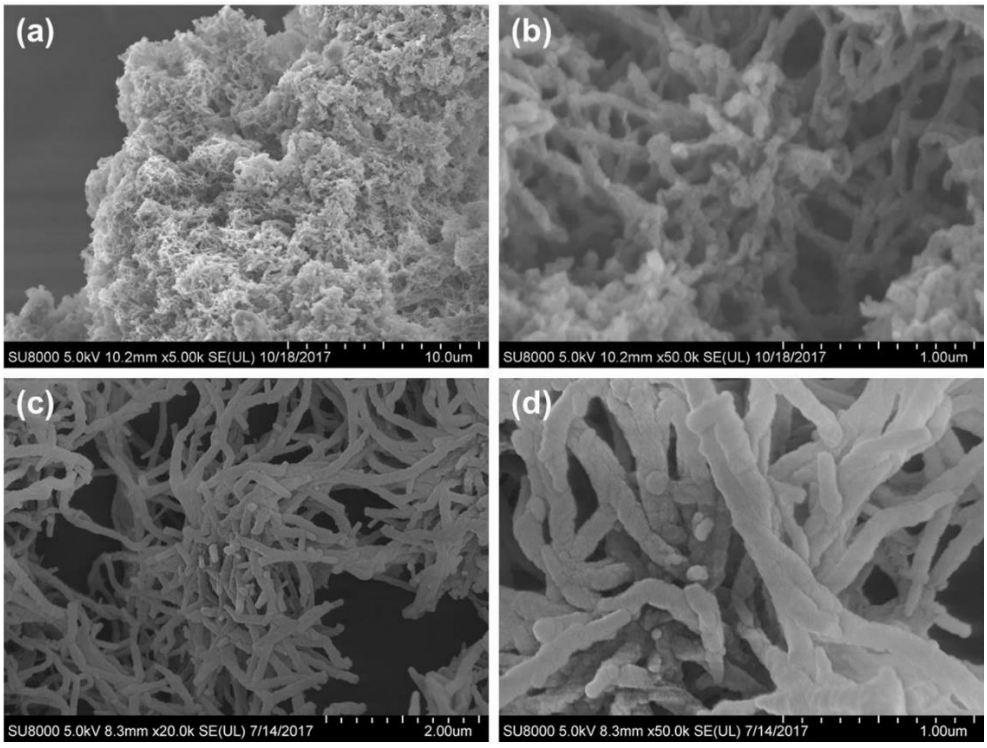

Figure S13. (a), (b) SEM images of **TPB-BT-COF** and (c), (d) **TAPT-BT-COF**. The images indicated that microstructures of both **BT-COFs** exhibited nanowire morphology.

Section 11. Transmission Electron Microscopy

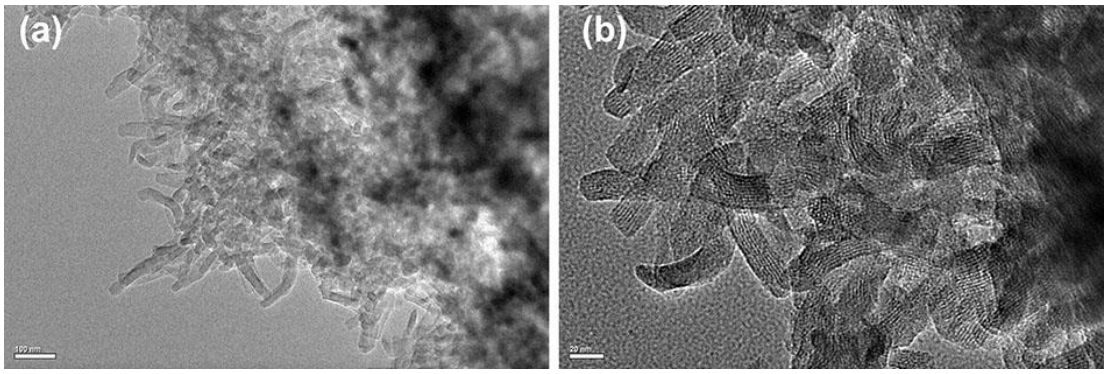

Figure S14. Representative TEM images of **TPB-BT-COF** (a) Low magnification image confirming the nanofibrillar structure and (b) HRTEM image showing fringes of periodicity.

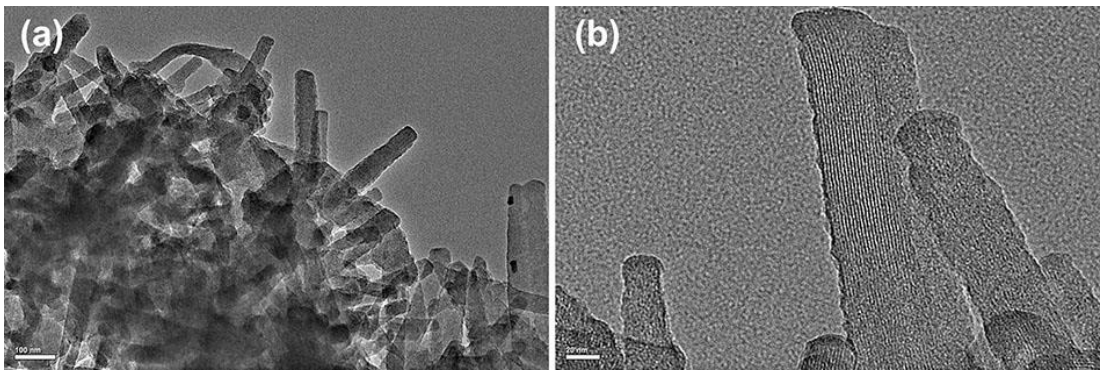

Figure S15. Representative TEM images of **TAPT-BT-COF** (a) Low magnification image confirming the nanofibrillar structure and (b) HR-TEM image showing fringes of periodicity.

Section 12. Electrochemical Properties of BT-COFs

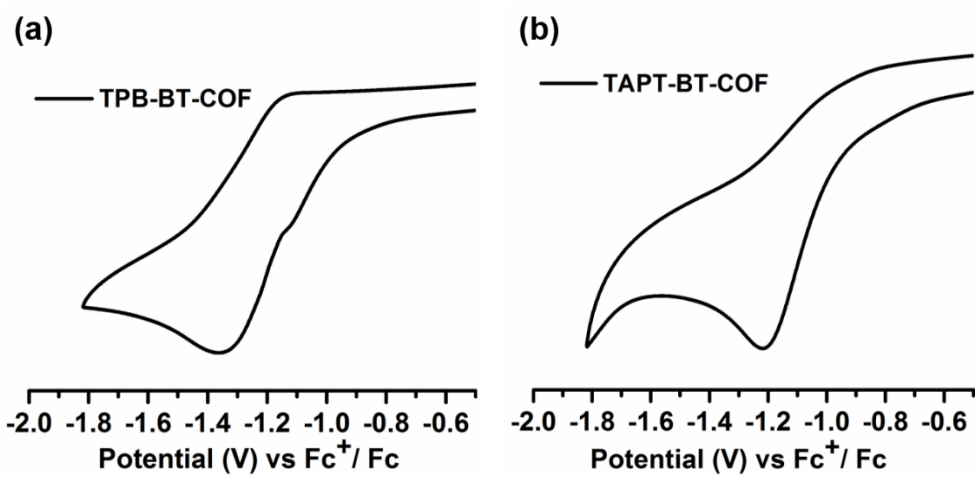

Figures S16. Cyclic voltammograms of BT-COFs**:** (a) **TPB-BT-COF** and (b) **TAPT-BT-COF**.

Table S2. Electrochemical properties of **TPB-BT-COF** and **TAPT-BT-COF**

BT-COFs	$E_{red\text{-}Onet}$ [V] [a]	CB [V] [c]	HOMO [eV] [b]	LUMO [eV] [b]	HOMO [eV] [d]	LUMO [eV] [d]	Band gap [eV] [d]	Band gap [eV]
TPB-BT-COF	-1.05	-0.41	-5.86	-3.75	-5.56	-4.21	1.35	2.05
TAPT-BT-COF	-0.94	-0.30	-5.99	-3.86	- 5.46	-3.85	1.61	2.13

[a]Ferrocene/ferrocenium redox-couple is used as reference. [b]The HOMO/LUMO levels are calculated according to the equations: $E_{LUMO} = -(4.8 + E_{red\text{-}onset})$ *eV.* $E_{HOMO} = E_{LUMO} - E_{gap}$*. [c]CB is conduction band; for conversion from Ferrocene/ferrocenium redox-couple to the Normal Hydrogen Electrode (NHE), the equation:* $E_{NHE} = E_{Fc/Fc^+} - 0.64$ *V is applied.*[S5] *[d]obtained by calculation at MS.7.0.*

Section 13. Photoreduction of Chromium (VI) to Chromium (III)

In a 10 ml of reaction tube, the porous monolith of COFs (*ca.* 10 mg) was added into 10 ml of Cr(VI) solution (10 mg/L). Firstly, the mixture was stirred constantly about 2 h for reaching adsorption and desorption equilibrium under Ar gas. Afterward, the mixture was illuminated with > 400 nm Xe lamp light source. 1 mL of Cr(VI) solution after photocatalytic reduction was mixed with H_2SO_4 (9 mL, 0.2 M), and then 0.2 mL of freshly prepared 0.25% (w/v) DPC in acetone was added. After the mixture were stirred for ca. 1 min, and was allowed to keep *ca.* 15 min. The obtained purple color was then measured at *ca.* 540 nm in UV-vis spectroscopy.[S5]

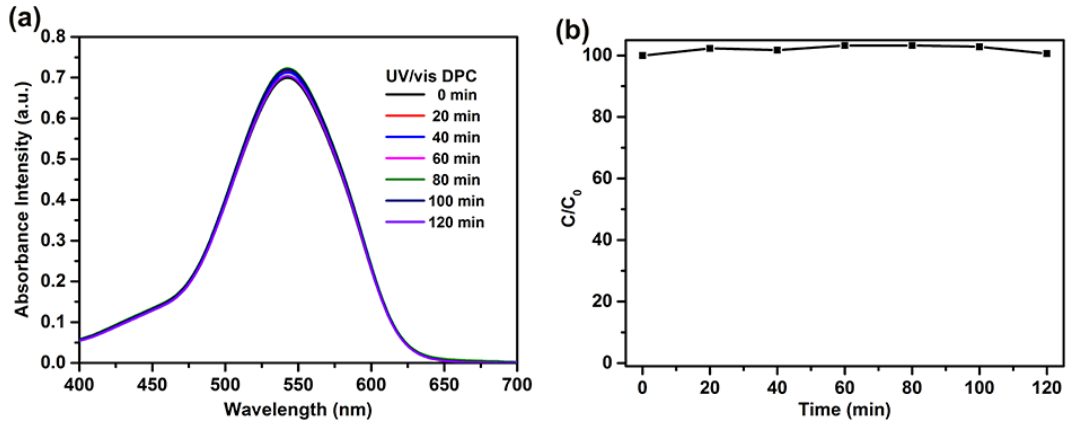

Figure S17. (a) UV-vis spectra and (b) concentration monitoring of the control experiment of using same light irradiation conditions but without BT-COF catalysts. C is the concentration of Cr(VI) after irradiation for different time and C_0 is the initial concentration.

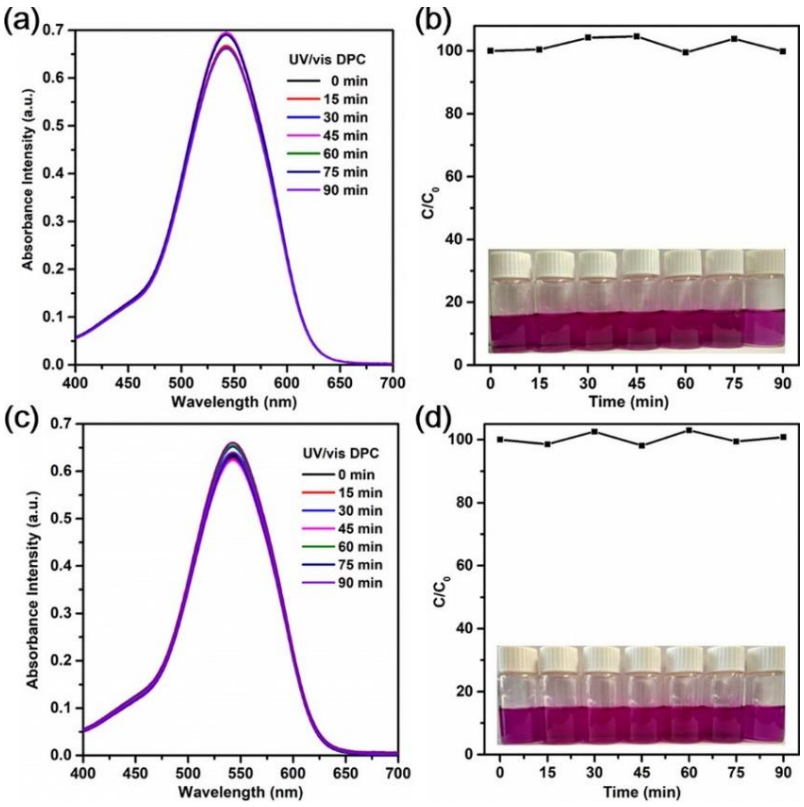

Figure S18. UV-vis spectra monitoring of DPC for determination of the adsorption of Cr (VI) onto (a) TPB-BT-COF and (c) TAPT-BT-COF in dark; The concentration variation of Cr (VI) upon adsorption onto (b) TPB-BT-COF and (d) TAPT-BT-COF in dark. Negligible removal of Cr(VI) by physical adsorption was observed. These results indicated that the photocatalytic reduction effect mainly contributed to the removal of Cr(VI).

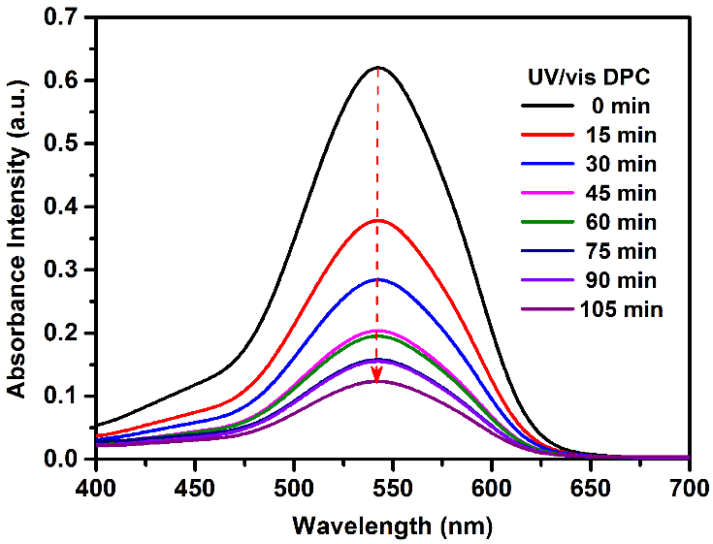

Figure S19. UV/vis absorption of DPC for determination of the photocatalytic reduction Cr(VI) to Cr(III) using TPB-TP-COF as photocatalyst in water under visible light irradiation.

Figure S20. The color change of DPC for determination of the photocatalytic reduction Cr(VI) to Cr(III) using TPB-TP-COF as photocatalyst in water under > 400nm Xe lamp light source irradiation.

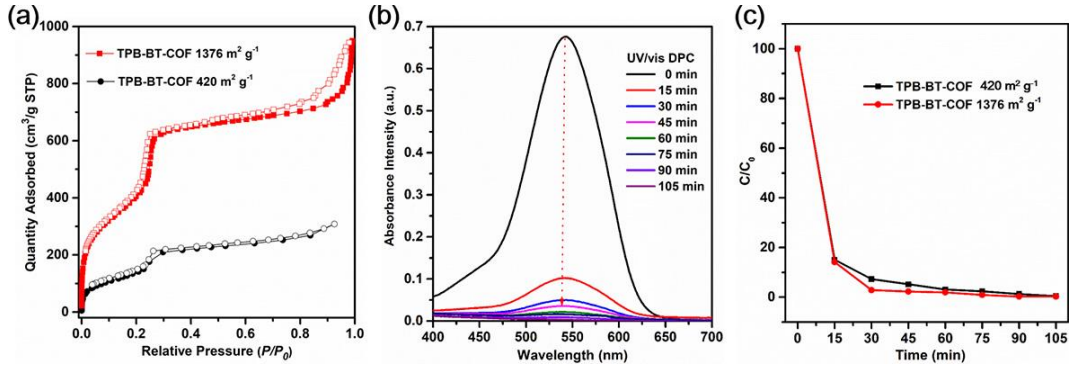

Figure S21. (a) Nitrogen-sorption isotherms of TPB-BT-COFs with different surface areas; (b) UV/vis absorption of DPC for determination of the photocatalytic reduction Cr(VI) to Cr(III) using less porous TPB-TP-COF (420 m^2 g^{-1}) as photocatalyst in water under visible light irradiation; (c) The photocatalytic rate comparison of TPB-TP-COF with different porosity, which indicate the porosity has negligible effect on the photocatalytic performance.

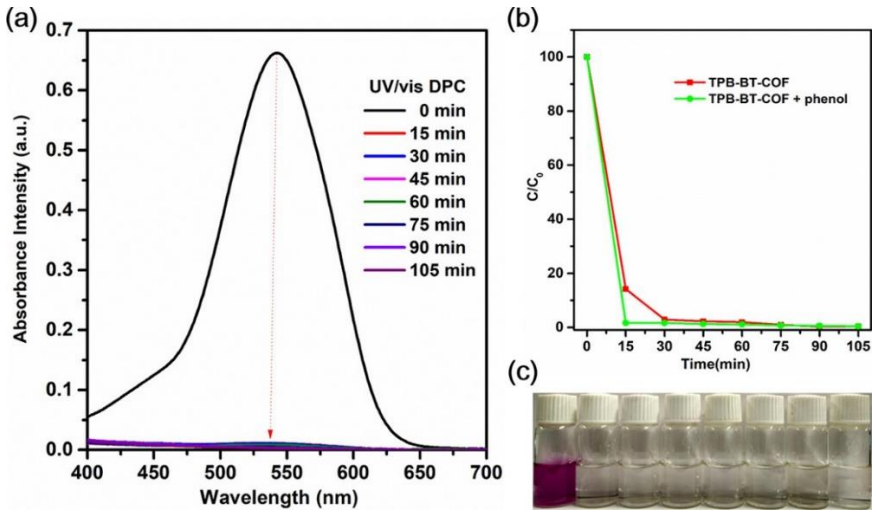

Figure S22. (a) UV/vis absorption of DPC for determination of the photocatalytic reduction Cr(VI) to Cr(III) using TPB-BT-COF with addition of the h^+ scavenger: phenol in water under visible light irradiation; (b) The photocatalytic rate comparison of TPB-BT-COF with and without addition of the h^+ scavenger: phenol; (c) Photograph of photocatalytic reduction using TPB-BT-COF with addition of phenol.

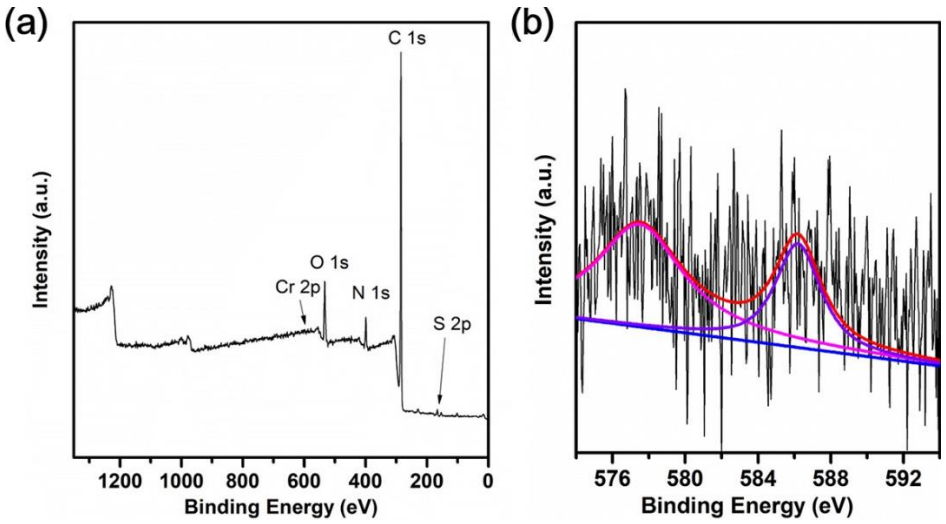

Figure S23. (a) XPS survey spectra and (b) high-resolution XPS spectra of TAPT-BT-COF after 1 cycles of photocatalysis. The two peaks at 576.7 and 586.2 eV are assigned to the $2p_{3/2}$ and $2p_{1/2}$ of Cr (III), which further confirmed the reduction of Cr (VI) to Cr (III).[S6,S7]

Section 14. Recycling Experiments

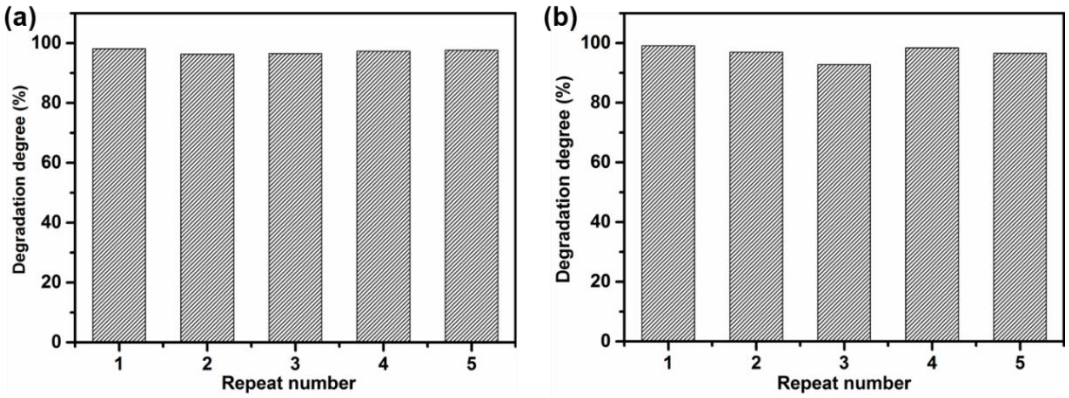

Figure S24. Recycling experiments of the photocatalytic reduction of Cr(VI) using BT-COFs in water under visible light irradiation: (a) **TPB-BT-COF**; and (b) **TAPT-BT-COF**.

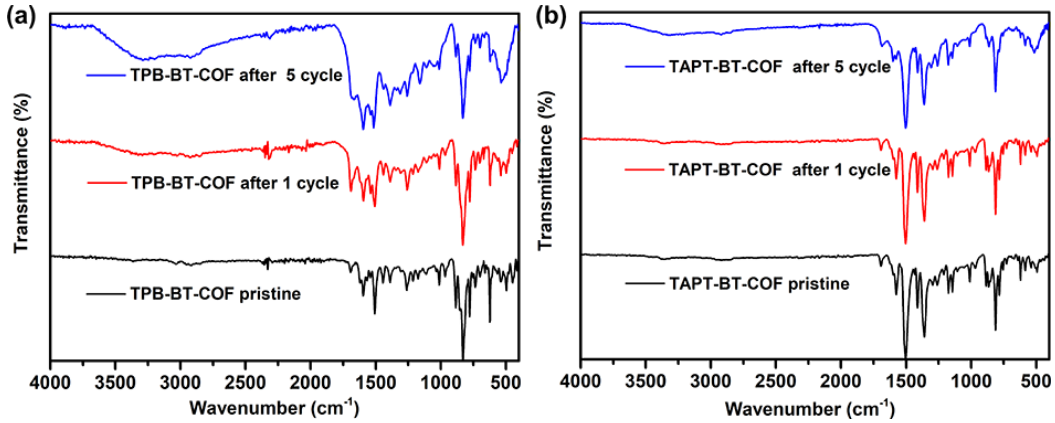

Figure S25. FT-IR spectra of a) **TPB-BT-COF** and b) **TAPT-BT-COF** at different cycle number under visible light irradiation.

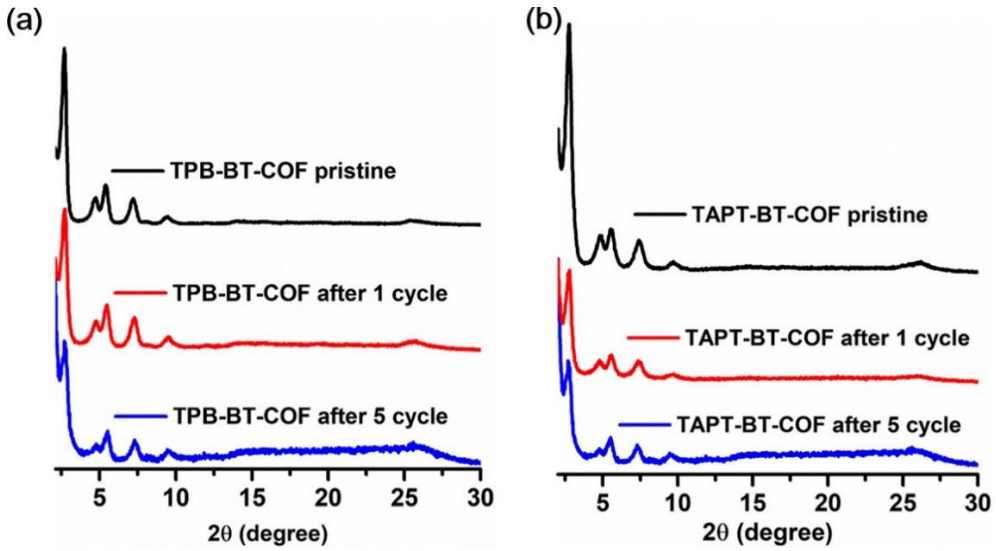

Figure S26. PXRD pattern comparison of a) **TPB-BT-COF** and b) **TAPT-BT-COF** before and after photocatalysis showing retention of crystallinity.

Section 15. •OH Radicals Test

The ·OH radical reactions were performed as follows: **BT-COFs** (5 mg) was suspended 8 mL aqueous solution containing 10 mM of NaOH and 5 mM of terephthalic acid (TA). The suspension was stirred in the dark for 30 min before exposing to visible light irradiation. After irradiated under visible light for 20 min, the mixture was centrifuged for fluorescence spectroscopy measurements. A fluorescence spectrophotometer was used to measure the fluorescence of the *in-situ* generated 2-hydroxy-terephthalic acid (TAOH). The excitation light wavelength used in recording fluorescence spectra was 320 nm.

Section 16. The Photocatalytic Performance Comparison

Table S3. The photocatalytic performance comparison of **BT-COFs** with other reported photocatalysts.

Type	Catalyst	Concentration of Cr(VI) ions	Irradiation time (min)	hole scavenger agents	pH value	degradation degree	Ref
Polymer	**TPB-BT-COF**	10 mg/L	75	no	pH = 7	99%	**Current work**
	TAPT-BT-COF	10 mg/L	105	no	pH = 7	99%	
	TPB-TP-COF	10 mg/L	105	no	pH = 7	80%	
	Phlo-POF	6 mg/L	60	no	pH=3	100%	S8
	P-FL-BT-3	25mg/L	120	no	pH = 7	100%	S9
	g-C_3N_4	10 mg/L	180	no	pH = 3	50%	S10
MOF	**NNU-36**	10 mg/L	60	CH_3OH	pH=2.17	95.3%	S11
	Pd@UiO-66(NH_2)	10 mg/L	90	no	pH=2	99%	S11
	RGO-UiO-66(NH_2)	10 mg/L	100	no	pH=7	100%	S12
	UiO-66(NH_2)	10 mg/L	100	no	pH=7	32%	S12
	MIL-	20 mg/L	180	EtOH	pH=2	97%	S13

	68(In)-NH_2 MIL-68(In)	20 mg/L	180	EtOH	pH=2	0%	S14
Inorganic Materials	**AgBr-hexagonal**	15 mg/L	80	no	pH = 7	66%	S15
	(AgIn)xZn2(1-x)S_2 /Ag_2S	--	90	no	pH = 7	99%	S7
	Ag_2S–Ag (H-2)	10 mg/L	80	no	pH = 7		S16
	TiO_2	20 mg/L	60	no	pH = 7	80%	S17
	MCRCSs	30 mg/L	120	no	pH=2	100%	S18
	$BiVO_4$/Bi_2S_3 (H-3)	10 mg/L	60	no	pH = 7	91.2%	S19

Section 17. Calculated Molecular Orbitals and Staggered AB Packing Modes

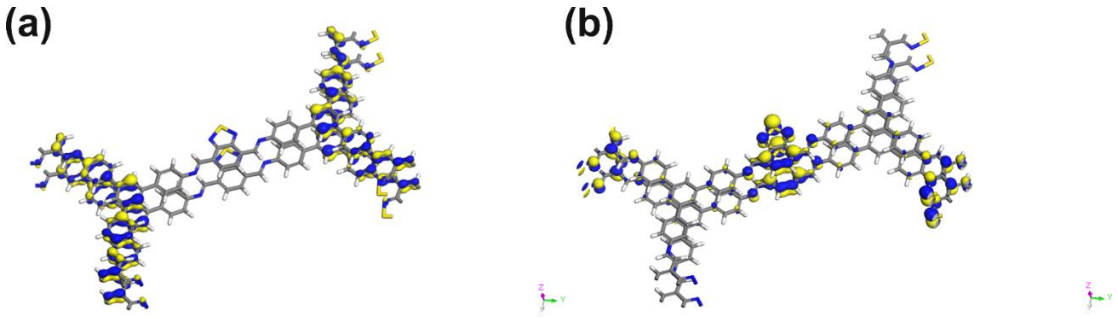

Figure S27. Calculated (a) HOMO and (b) LUMO of **TPB-BT-COF** for -5.5658 eV and -4.2055 eV, respectively. In the calculated HOMO of the repeating unit of the framework of **TPB-BT-COF**, electrons are delocalized over the two TPB segments; while in the LUMO, electrons are mainly distributed in the BT units. This results clearly demonstrated that TPB moiety served as the donor, whereas the BT unit works as the acceptor in the D-A framework skeleton. This structure is well known to be beneficial for intramolecular charge transfer and charge separation upon photoexcitation.

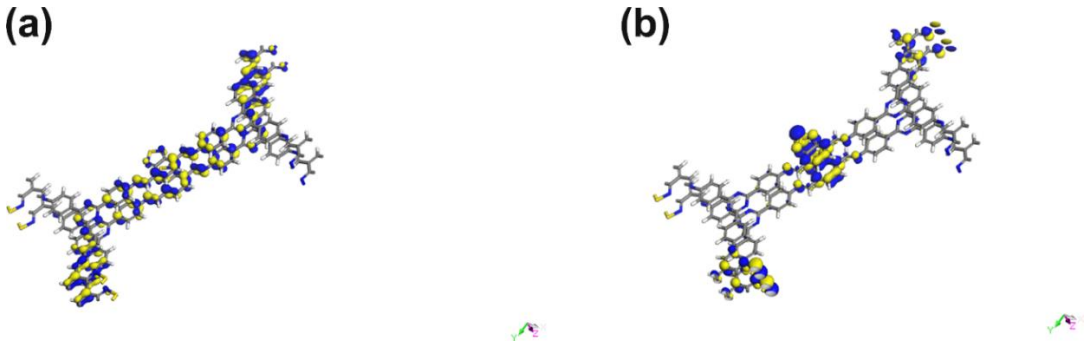

Figure S28. Calculated (a) HOMO and (b) LUMO of **TAPT-BT-COF** for - 5.4633 eV and -3.8508 eV, respectively. In the calculated HOMO of the repeating unit of **TAPT-BT-COF**, electrons are delocalized over almost the whole skeletons; while in the LUMO, electrons are mainly distributed in the BT units. These results indicated that **TAPT-BT-COF** did own intramolecular charge transfer effect but is much less effective compared to that of **TPB-BT-COF**.

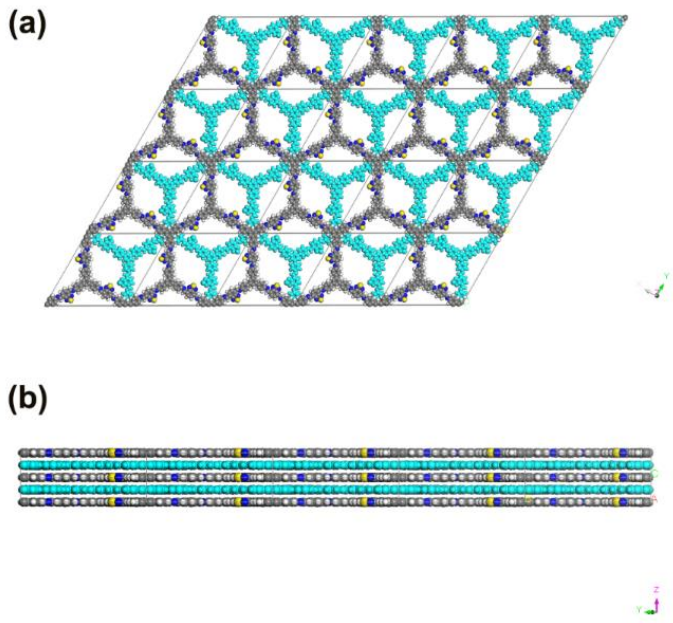

Figure S29. (a) Top-view and (b) Side-view of the **TPB-BT-COF** in staggered AB stacking modes.

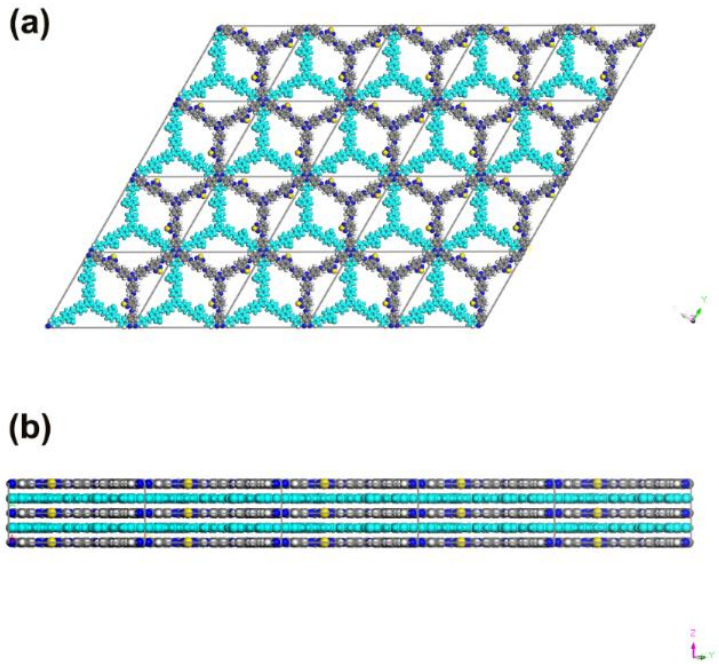

Figure S30. (a) Top-view and (b) Side-view of the **TAPT-BT-COF** in staggered AB stacking modes.

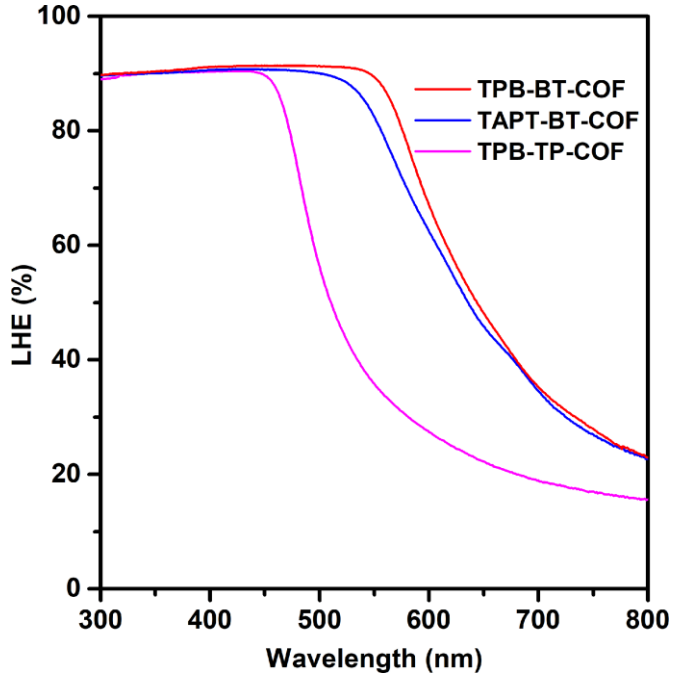

Figure S31. The light harvesting efficiency (LHE) spectra of **TPB-BT-COF** (red), **TAPT-BT-COF** (blue) and **TPB-TP-COF** (magenta) from UV−vis absorption spectra. The light harvesting efficiency (LHE) was defined as LHE = $1\text{-}10^{-A}$ (A is absorbance obtained from the UV–vis measurement).

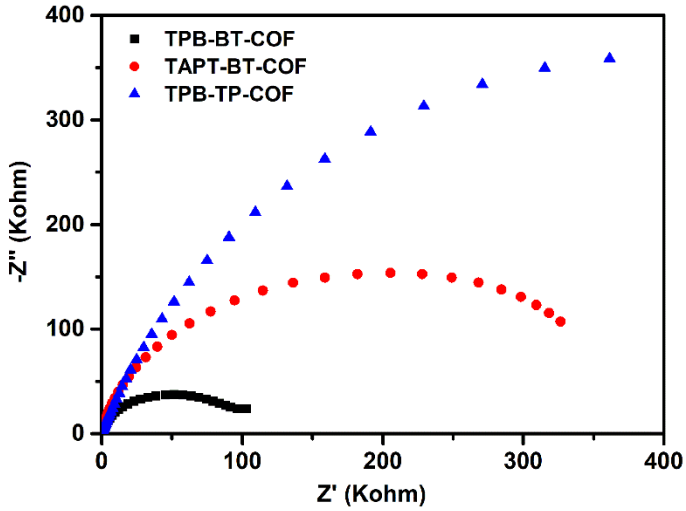

Figure S32. Electrochemical impedance spectra of TPB-BT-COF (black line), TAPT-BT-COF (red line) and TPB-TP-COF (black line) under visible light irradiation.

Table S4. Atomic coordinates of AA-stacking mode of **TPB-BT-COF** using DFTB+ method.

Space group: *P*6 **a = 37.9853 Å, b = 37.9853 Å, and c = 3.4885 Å.** **$\alpha = \beta = 90°$, and $\gamma = 120°$**			
	X	**Y**	**Z**
C	1.48667	-0.97193	-0.50000
C	1.45868	-1.01390	-0.50000
C	1.47223	-1.04232	-0.50000
C	1.51448	-1.02716	-0.50000
C	1.54160	-0.98630	-0.50000
C	1.52883	-0.95752	-0.50000
C	1.55881	-0.91359	-0.50000
C	1.31071	-0.37554	-0.50000
C	1.35350	-0.35664	-0.50000
C	1.24347	-0.37502	-0.50000
C	1.22225	-0.35307	-0.50000
C	1.17980	-0.37296	-0.50000
C	1.15666	-0.41515	-0.50000
C	1.17667	-0.43770	-0.50000
C	1.21916	-0.41808	-0.50000
C	1.44200	-0.08624	-0.50000
N	1.45348	-0.11320	-0.50000
C	1.68631	-0.68923	-0.50000

C	1.71015	-0.64643	-0.50000
C	1.61861	-0.75654	-0.50000
C	1.57545	-0.77783	-0.50000
C	1.55295	-0.82029	-0.50000
C	1.57206	-0.84339	-0.50000
C	1.61464	-0.82326	-0.50000
C	1.63743	-0.78078	-0.50000
N	1.54687	-0.88693	-0.50000
N	1.41765	-0.53275	-0.50000
S	1.39575	-0.58405	-0.50000
N	1.44200	-0.58047	-0.50000
H	1.47551	-0.95066	-0.50000
H	1.42645	-1.02415	-0.50000
H	1.59069	-0.90444	-0.50000
H	1.29348	-0.40768	-0.50000
H	1.23717	-0.32047	-0.50000
H	1.16443	-0.35543	-0.50000
H	1.16003	-0.47048	-0.50000
H	1.23167	-0.43793	-0.50000
H	1.41020	-0.09513	-0.50000
H	1.70128	-0.70641	-0.50000
H	1.55772	-0.76296	-0.50000
H	1.52008	-0.83560	-0.50000

H	1.63088	-0.83979	-0.50000
H	1.66980	-0.76821	-0.50000

Table S5. Atomic coordinates of staggered AB-stacking mode of **TPB-BT-COF** using DFTB+ method.

Space group: *P*6 **a = 37.6121 Å, b = 37.6121 Å, and c = 6.3664 Å.** **$\alpha = \beta = 90°$, and $\gamma = 120°$**			
	X	**Y**	**Z**
C	-0.17945	-0.30527	0.00000
C	-0.20702	0.65191	0.00000
C	-0.19403	0.62325	0.00000
C	-0.14981	0.63712	-0.00000
C	-0.12142	-0.31777	0.00000
C	-0.13702	-0.28923	0.00000
C	-0.10806	-0.24540	0.00000
C	-0.35616	0.29060	0.00000
C	-0.31325	0.31009	0.00000
C	-0.42230	0.29288	0.00000
C	-0.44349	0.31479	0.00000
C	-0.48640	0.29540	0.00000

C	-0.50967	0.25191	0.00000
C	-0.48930	0.22906	0.00000
C	-0.44633	0.24921	0.00000
C	-0.22381	0.57937	0.00000
N	-0.21147	0.55249	-0.00000
C	0.01961	-0.02324	0.00000
C	0.04355	0.02026	0.00000
C	-0.04812	-0.08922	0.00000
C	-0.09181	-0.10964	0.00000
C	-0.11484	-0.15234	0.00000
C	-0.09567	-0.17648	0.00000
C	-0.05228	-0.15666	0.00000
C	-0.02936	-0.11373	0.00000
N	-0.12124	-0.21907	0.00000
N	-0.25224	0.13456	0.00000
S	-0.27306	0.07896	0.00000
N	-0.22332	0.08183	0.00000
H	-0.19188	-0.28426	0.00000
H	-0.23995	0.64113	0.00000
H	-0.07476	-0.23584	0.00000
H	-0.37464	0.25725	0.00000
H	-0.42638	0.34843	0.00000
H	-0.50156	0.31415	0.00000

H	-0.50689	0.19568	0.00000
H	-0.43268	0.22947	0.00000
H	-0.25730	0.57041	0.00000
H	0.03527	-0.04172	0.00000
H	-0.10874	-0.09280	0.00000
H	-0.14798	-0.16778	0.00000
H	-0.03517	-0.17319	0.00000
H	0.00413	-0.09899	0.00000
C	1.15394	0.36129	0.50000
C	1.12631	1.31836	0.50000
C	1.13931	1.28974	0.50000
C	1.18349	1.30369	0.50000
C	1.21191	0.34871	0.50000
C	1.19634	0.37745	0.50000
C	1.22530	0.42128	0.50000
C	0.97724	0.95728	0.50000
C	1.02009	0.97676	0.50000
C	0.91086	0.95947	0.50000
C	0.88974	0.98146	0.50000
C	0.84677	0.96202	0.50000
C	0.82389	0.91851	0.50000
C	0.84430	0.89574	0.50000
C	0.88708	0.91580	0.50000

C	1.10954	1.24584	0.50000
N	1.12170	1.21890	0.50000
C	1.35294	0.64340	0.50000
C	1.37678	0.68673	0.50000
C	1.28532	0.57778	0.50000
C	1.24168	0.55703	0.50000
C	1.21854	0.51410	0.50000
C	1.23767	0.48994	0.50000
C	1.28116	0.51011	0.50000
C	1.30394	0.55305	0.50000
N	1.21172	0.44719	0.50000
N	1.08094	0.80135	0.50000
S	1.06025	0.74576	0.50000
N	1.10991	0.74850	0.50000
H	1.14157	0.38229	0.50000
H	1.09338	1.30775	0.50000
H	1.25865	0.43062	0.50000
H	0.95867	0.92396	0.50000
H	0.90729	1.01523	0.50000
H	0.83202	0.98087	0.50000
H	0.82667	0.86253	0.50000
H	0.90078	0.89625	0.50000
H	1.07608	1.23698	0.50000

H	1.36867	0.62497	0.50000
H	1.22450	0.57371	0.50000
H	1.18510	0.49861	0.50000
H	1.29817	0.49313	0.50000
H	1.33733	0.56735	0.50000

Table S6. Atomic coordinates of AA-stacking mode of **TAPT-BT-COF** using DFTB+ method.

Space group: *P*6 **a = 37.4830 Å, b = 37.4830 Å, and c = 3.4950 Å.** **$\alpha = \beta = 90°$, and $\gamma = 120°$**			
	X	**Y**	**Z**
C	1.55903	-0.91161	-0.50000
N	1.31079	-0.37541	-0.50000
C	1.35239	-0.35542	-0.50000
C	1.24632	-0.37366	-0.50000
C	1.22527	-0.35120	-0.50000
C	1.18235	-0.37103	-0.50000
C	1.15810	-0.41462	-0.50000
C	1.17920	-0.43715	-0.50000
C	1.22211	-0.41713	-0.50000
C	1.51471	-0.02916	-0.50000
C	1.54359	0.01507	-0.50000

C	1.52911	0.04424	-0.50000
C	1.48660	0.02844	-0.50000
C	1.45841	-0.01441	-0.50000
C	1.47107	-0.04382	-0.50000
C	1.44140	-0.08806	-0.50000
N	1.45318	-0.11527	-0.50000
N	1.68629	-0.68921	-0.50000
C	1.70784	-0.64747	-0.50000
C	1.61999	-0.75369	-0.50000
C	1.57647	-0.77477	-0.50000
C	1.55365	-0.81769	-0.50000
C	1.57299	-0.84187	-0.50000
C	1.61664	-0.82078	-0.50000
C	1.63930	-0.77785	-0.50000
N	1.54692	-0.88467	-0.50000
N	1.41537	-0.53080	-0.50000
S	1.39318	-0.58637	-0.50000
N	1.44305	-0.58350	-0.50000
H	1.59237	-0.90329	-0.50000
H	1.24291	-0.31730	-0.50000
H	1.16660	-0.35291	-0.50000
H	1.16211	-0.47098	-0.50000
H	1.23736	-0.43571	-0.50000

H	1.47495	0.05010	-0.50000
H	1.42523	-0.02462	-0.50000
H	1.40800	-0.09632	-0.50000
H	1.56021	-0.75711	-0.50000
H	1.51977	-0.83326	-0.50000
H	1.63328	-0.83796	-0.50000
H	1.67315	-0.76262	-0.50000

Table S7. Atomic coordinates of staggered AB-stacking mode of **TAPT-BT-COF** using DFTB+ method.

Space group: *P*6 **a = 37.4830 Å, b = 37.4830 Å, and c = 3.4950 Å.** **$\alpha = \beta = 90°$, and $\gamma = 120°$**			
	X	**Y**	**Z**
C	-0.10751	-0.24423	0.50000
N	-0.35590	0.29123	0.50000
C	-0.31430	0.31133	0.50000
C	-0.42007	0.29309	0.50000
C	-0.44107	0.31561	0.50000
C	-0.48398	0.29556	0.50000
C	-0.50805	0.25194	0.50000
C	-0.48697	0.22930	0.50000
C	-0.44404	0.24961	0.50000

C	-0.15175	0.63740	0.50000
C	-0.12247	-0.31788	0.50000
C	-0.13711	-0.28865	0.50000
C	-0.17978	-0.30518	0.50000
C	-0.20801	0.65179	0.50000
C	-0.19577	0.62215	0.50000
C	-0.22596	0.57789	0.50000
N	-0.21403	0.55090	0.50000
N	0.01961	-0.02250	0.50000
C	0.04099	0.01910	0.50000
C	-0.04634	-0.08659	0.50000
C	-0.08982	-0.10734	0.50000
C	-0.11274	-0.15024	0.50000
C	-0.09335	-0.17445	0.50000
C	-0.04960	-0.15352	0.50000
C	-0.02689	-0.11058	0.50000
N	-0.11970	-0.21738	0.50000
N	-0.25143	0.13533	0.50000
S	-0.27385	0.07962	0.50000
N	-0.22378	0.08278	0.50000
H	-0.07422	-0.23564	0.50000
H	-0.42318	0.34954	0.50000
H	-0.49970	0.31373	0.50000

H	-0.50423	0.19540	0.50000
H	-0.42834	0.23139	0.50000
H	-0.19222	-0.28408	0.50000
H	-0.24115	0.64165	0.50000
H	-0.25935	0.56948	0.50000
H	-0.10570	-0.08929	0.50000
H	-0.14662	-0.16588	0.50000
H	-0.03296	-0.17076	0.50000
H	0.00704	-0.09489	0.50000
C	1.22575	0.42230	1.00000
N	0.97743	0.95790	1.00000
C	1.01901	0.97801	1.00000
C	0.91337	0.95981	1.00000
C	0.89244	0.98238	1.00000
C	0.84952	0.96232	1.00000
C	0.82547	0.91868	1.00000
C	0.84654	0.89603	1.00000
C	0.88948	0.91633	1.00000
C	1.18152	1.30395	1.00000
C	1.21082	0.34866	1.00000
C	1.19618	0.37788	1.00000
C	1.15352	0.36137	1.00000
C	1.12528	1.31835	1.00000

C	1.13751	1.28869	1.00000
C	1.10731	1.24442	1.00000
N	1.11919	1.21740	1.00000
N	1.35294	0.64417	1.00000
C	1.37436	0.68578	1.00000
C	1.28694	0.57998	1.00000
C	1.24344	0.55915	1.00000
C	1.22050	0.51624	1.00000
C	1.23986	0.49203	1.00000
C	1.28360	0.51297	1.00000
C	1.30633	0.55591	1.00000
N	1.21352	0.44911	1.00000
N	1.08183	0.80206	1.00000
S	1.05940	0.74635	1.00000
N	1.10947	0.74949	1.00000
H	1.25907	0.43094	1.00000
H	0.91035	1.01631	1.00000
H	0.83381	0.98049	1.00000
H	0.82929	0.86213	1.00000
H	0.90519	0.89814	1.00000
H	1.14112	0.38252	1.00000
H	1.09215	1.30825	1.00000
H	1.07393	1.23606	1.00000

H	1.22754	0.57718	1.00000
H	1.18663	0.50060	1.00000
H	1.30025	0.49572	1.00000
H	1.34025	0.57158	1.00000

Section 18. Supporting References

S1. M. Li, H. Zhang, Y. Zhang, B. Hou, C. Li, X. Wang, J. Zhang, L. Xiao, Z. Cui and Y. Ao, *J. Mater. Chem. C*, 2016, **4**, 9094.

S2. M. G. Schwab, M. Hamburger, X. Feng, J. Shu, H. W. Spiess, X. Wang, M. Antonietti and K. Müllen, *Chem. Commun.*, 2010, **46**, 8932.

S3. P. Bhanja, K. Bhunia, S. K. Das, D. Pradhan, R. Kimura, Y. Hijikata, S. Irle and A. Bhaumik, *ChemSusChem*, 2017, **10**, 921-929.

S4. L.-H. Li, X.-L. Feng, X.-H. Cui, Y.-X. Ma, S.-Y. Ding and W. Wang, *J. Am. Chem. Soc.*, 2017, **139**, 6042.

S5. C. M. Cardona, W. Li, A. E. Kaifer, D. Stockdale and G. C. Bazan, *Adv. Mater.*, 2011, **23**, 2367.

S6. Y.-Z. Yan, Q.-D. An, Z.-Y. Xiao, S.-R. Zhai, B. Zhai and Z. Shi, *J. Mater. Chem. A*, 2017, **5**, 17073.

S7. H. Abdullah and D.-H. Kuo, *ACS Appl. Mater. Inter.*, 2015, **7**, 26941.

S8. V. Kostas, M. Baikousi, K. Dimos, K. C. Vasilopoulos, I. Koutselas and M. A. Karakassides, *J. Phys. Chem. C* **2017**, 2017, **121**, 7303.

S9. S. Ghasimi, S. Prescher, Z. J. Wang, K. Landfester, J. Yuan and K. A. I. Zhang, *Angew. Chem. Int. Ed.*, 2015, **54**, 14549.

S10. W. Huang, N. Liu, X. Zhang, M. Wu and L. Tang, *Appl. Surf. Sci.*, 2017, **425**, 107.

S11. H. Zhao, Q. Xia, H. Xing, D. Chen and H. Wang, *ACS Sustainable Chem. Eng.*, 2017, **5**, 4449.

S12. L. Shen, W. Wu, R. Liang, R. Lin and L. Wu, *Nanoscale*, 2013, **5**, 9374.

S13. L. Shen, L. Huang, S. Liang, R. Liang, N. Qin and L. Wu, *RSC Adv.*, 2014, **4**, 2546.

S14. R. Liang, L. Shen, F. Jing, W. Wu, N. Qin, R. Lin and L. Wu, *Applied Catalysis B: Environmental*, 2015, **162**, 245.

S15. H. Zheng, P. Li, L. Gao and G. Li, *RSC Adv.*, 2017, **7**, 25725.

S16. W. Yang, L. Zhang, Y. Hu, Y. Zhong, H. B. Wu and X. W. Lou, *Angew. Chem. Int. Ed.*, 2012, **51**, 11501.

S17.Q. Liu, B. Zhou, M. Xu and G. Mao, *RSC Adv.*, 2017, **7**, 8004.

S18. Z. Luo, J. Wang, L. Qu, J. Jia, S. Jiang, X. Zhou, X. Wu and Z. Wu, *New J. Chem.*, 2017, **41**, 12596.

S19. X. Gao, H. B. Wu, L. Zheng, Y. Zhong, Y. Hu and X. W. Lou, *Angew. Chem. Int. Ed*., 2014, **53**, 5917.